Immunity 24, 601–610, May 2006 ©2006 Elsevier Inc. DOI 10.1016/j.immuni.2006.03.012

Carbon Monoxide Orchestrates a Protective Response through PPARγ

Martin Bilban,[1,3] Fritz H. Bach,[1] Sherrie L. Otterbein,[4] Emeka Ifedigbo,[4] Joana de Costa d'Avila,[1] Harald Esterbauer,[3] Beek Yoke Chin,[1] Anny Usheva,[2] Simon C. Robson,[2] Oswald Wagner,[3,5] and Leo E. Otterbein[1,5,*]
[1] Department of Surgery
[2] Department of Medicine
Beth Israel Deaconess Medical Center
Harvard Medical School
Boston, Massachusetts 02215
[3] Department of Laboratory Medicine
Medical University of Vienna
Ludwig Boltzmann Institute for Clinical and Experimental Oncology
A-1090 Vienna
Austria
[4] Department of Medicine
University of Pittsburgh School of Medicine
Pittsburgh, Pennsylvania 15213

Summary

Carbon monoxide (CO) suppresses proinflammatory responses in macrophages reacting to LPS. We hypothesize that CO acts by inducing a molecule(s) that suppresses the inflammatory response to subsequent stress. Exposure of macrophages to CO alone in vitro produced a brief burst of mitochondrial-derived ROS, which led to expression of PPARγ. PPARγ expression proved essential for mediating the anti-inflammatory effects of CO. Blocking the CO-mediated increase in ROS generation prevented PPARγ induction, and blocking PPARγ prevented CO's anti-inflammatory effects. In a model of acute lung injury in mice, CO blocked expression of Egr-1, a central mediator of inflammation, and decreased tissue damage; inhibition of PPARγ abrogated both effects. These data identify the mitochondrial oxidases as an (perhaps the) initial cellular target of CO and demonstrate that CO upregulates expression of PPARγ via the mitochondria, which assures that a subsequent stress stimulus will lead to a cytoprotective as opposed to a proinflammatory phenotype.

Introduction

Pretreatment of cells or animals with low concentrations of carbon monoxide (CO) exerts anti-inflammatory effects in a number of models (Otterbein et al., 2000; Sarady et al., 2004; Fujita et al., 2001; Otterbein et al., 2003a; Zuckerbraun et al., 2003). As an example, macrophages mount a proinflammatory response to LPS; with CO treatment initiated either before or after LPS (Otterbein et al., 2000; Sarady et al., 2004), the proinflammatory response is suppressed and the production of IL-10, an anti-inflammatory cytokine, is boosted. A significant body of knowledge has been gained about the signaling pathways involved in these effects. What has not been investigated is whether CO exposure alone modulates the molecular machinery of macrophages so that a subsequent stress stimulus will elicit an anti-inflammatory as opposed to a proinflammatory response. We hypothesize that CO mediates its effects by upregulating a molecule (or molecules) in the macrophage that, by virtue of its presence, modulates the later molecular response to a stress stimulus. To gain insight into differential gene expression patterns, we initially employed gene chip technology and then related candidate genes to their involvement in modulating the inflammatory response. One of the genes that emerged was peroxisome proliferator-activated receptor-γ (PPARγ). PPARγ is a nuclear hormone receptor expressed in monocytes and macrophages, where it plays a critical role in regulating the expression of genes involved in inflammatory signaling (Welch et al., 2003; reviewed in Delerive et al., 2001; Gelman et al., 2005). The molecular mechanisms by which PPARγ dampens the macrophage inflammatory responses are thought to be mediated by inhibition of expression of proinflammatory molecules such as TNFα, IL-6, IL-1β, IP-10, and iNOS (Ricote et al., 1998; Welch et al., 2003).

Given that CO is known to bind to oxidases (hemoproteins) in the mitochondria, we examined the effects of CO on the generation of reactive oxygen species (ROS). We show that exposure to CO leads to a rapid and brief burst of ROS from the mitochondria that directs the subsequent upregulation of PPARγ. Both events prove essential for the anti-inflammatory effects of CO both in vitro and in vivo. These findings provide us with our first understanding of the early cellular response to CO that is involved in the mediation of its anti-inflammatory effects.

Results

CO Suppresses LPS-Induced Egr-1 mRNA and Protein Expression via PPARγ

Preliminary microarray studies (Figures S2 and S3 and Table S1) showed that CO strongly suppressed Egr-1 mRNA and protein expression in macrophages treated with 100 ng/ml of LPS as compared to cells stimulated in the absence of CO (Figures 1A–1C). CO exposure also prevented Egr-1/DNA binding in nuclear extracts of LPS-treated cells (Figure 1D). We evaluated a potential role for PPARγ, which suppresses ischemia-induced Egr-1 in alveolar macrophages, in the anti-inflammatory effects of CO (Okada et al., 2002). Inhibition of PPARγ with its selective inhibitor GW9662 added prior to CO did not affect Egr-1 expression in LPS-stimulated cells. However, blocking of PPARγ did block the suppressive effect of CO seen in the absence of the PPARγ inhibitor (Figure 1E). Similarly, experiments using siRNA to specifically inhibit PPARγ (Figure 1F and Figure S1) demonstrated that the ability of CO to block Egr-1 induction was PPARγ dependent. Figure 1G depicts the

*Correspondence: lotterbe@bidmc.harvard.edu
[5] These authors contributed equally to this work.

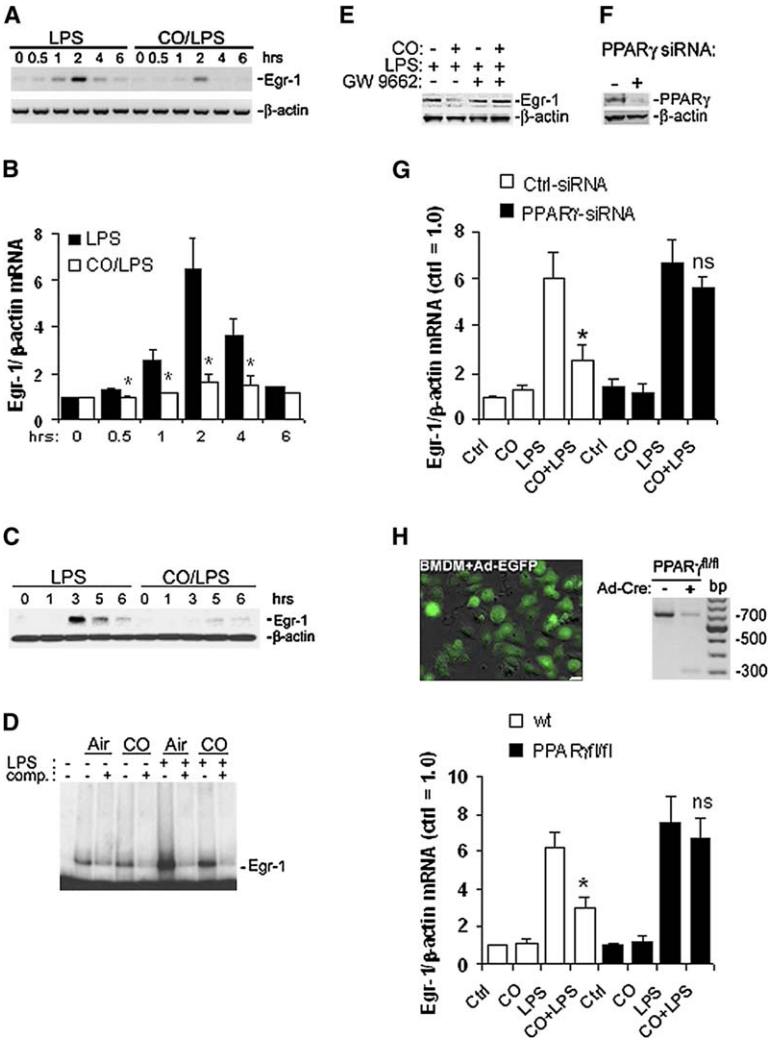

Figure 1. CO Inhibits Egr-1 Expression/Function via PPARγ in Macrophages

(A) RAW cells were stimulated with LPS (100 pg/ml) in the presence or absence of 250 ppm CO. Egr-1 mRNA was analyzed by RT-PCR. One representative agarose gel is shown.

(B) Quantitative densitometric data are expressed as Egr-1/β-actin mRNA levels. Data are mean (n = 3) ± SD (*p < 0.05 versus LPS).

(C) Egr-1 protein expression. β-actin demonstrates equal protein loading.

(D) EMSA for Egr-1 on nuclear extracts of cells treated with CO or air followed by stimulation with LPS for 1 hr. The left-most lane is Egr-1-free probe. Migration of the band corresponding to the Egr-1-DNA complex is indicated on the right. Egr-1 specificity of the protein-DNA interaction was shown by competition experiments in which a 100-fold molar excess of unlabeled Egr-1 probe obliterated the appearance of the gel shift band (marked as "competitor: +").

(E) RAW cells were pretreated with GW9662 (2 μM) followed by treatment with or without CO. LPS was then added and expression assessed by Western blotting. The blot is representative of four independent experiments.

(F) To inhibit endogenous PPARγ expression, RAW cells were transfected with a PPARγ-specific siRNA (see Figure S1 for specificity and sequences tested). PPARγ protein levels were determined 48 hr later by Western blotting. The blot is representative of three independent experiments.

(G) RAW cells were transfected with control (open bars) or PPARγ-specific siRNA (filled bars) followed by a 3 hr pretreatment with or without CO 48 hr later. LPS was then added, and expression analyzed by real-time-PCR. Quantitation of siRNA experiments is expressed as Egr-1 mRNA normalized to β-actin and nonstimulated siRNA-transfected controls. Data are mean (n = 3) ± SD (*p < 0.05 versus LPS/ctrl-siRNA; ns, not significant versus LPS/PPARγ-siRNA).

(H) Differentiated BMDM from PPARγ-loxP mice (B6.129-Pparg$^{tm2Rev/J}$) or BMDM isolated from wild-type controls (open bars) were infected with adeno-*Cre* recombinase for 36–48 hr. Efficiency of infection was determined with Adeno-EGFP, and confirmation of recombination was performed by semiquantitative RT-PCR-detecting floxed-out exons 1 and 2 (~300 bp; upper panel) in the adeno-*Cre*-treated cells. LPS was then added to the media in the presence or absence of CO (250 ppm), and Egr-1 expression was measured 1 hr later by RT-PCR as described in (G). Note that CO blocked LPS-induced Egr-1 in control-infected BMDM but was not able to block in those cells infected with adeno-*Cre* recombinase where PPARγ expression was disrupted through *Cre*-mediated recombination of the PPARγ floxed exons 1 and 2.

quantitative analyses of the siRNA experiments. The siRNA did not inhibit LPS-induced Egr-1. The role of PPARγ in mediating the CO effects was further investigated with a *Cre*/lox system. Bone marrow derived macrophages were prepared as described in Experimental Procedures from wild-type and PPARγ-loxP mice and infected with an adenovirus expressing *Cre* recombinase. Recombination and knockdown was verified in these cells, and >95% efficiency of infection was observed (Figure 1H, upper panels). These cells were treated with LPS in the presence and absence of CO, and Egr-1 expression was measured by real-time PCR. As shown in Figure 1H, LPS induced a significant increase in Egr-1 expression in Ad-*Cre*-treated wild-type cells, which was blocked in the presence of CO. In the Ad-*Cre*-infected PPARγ-loxP cells in which PPARγ was knocked down, CO was unable to inhibit LPS-induced Egr-1. These experiments confirm the ones using siRNA as well as those using the selective PPARγ inhibitor. These data demonstrate that the ability of CO to suppress Egr-1 expression in response to LPS is dependent on the activation of PPARγ.

CO Increases Nuclear PPARγ that Inhibits LPS-Induced Elk-1 Activation

Exposure of RAW cells to CO for 2–4 hr resulted in an increase in nuclear PPARγ demonstrated by immunofluorescence staining, Western blotting, and reporter assays (Figures 2A–2C). Because LPS induces Egr-1 activation via phosphorylation of the transcription factor Elk-1 (Guha et al., 2001), we investigated whether PPARγ modulates LPS-induced Elk-1 phosphorylation. Phosphorylation of Elk-1 was barely detectable in untreated cells; addition of LPS resulted in a rapid increase

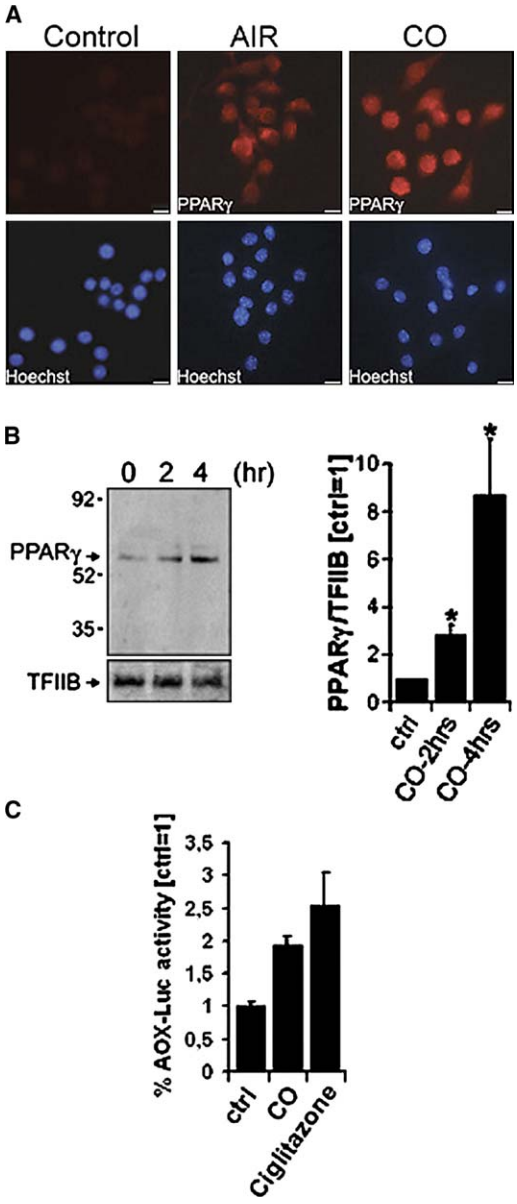

Figure 2. CO Increases Nuclear PPARγ Expression and Activity

(A) RAW 264.7 cells were exposed to air or CO (4 hr) and immunostained for PPARγ. The image is representative of three experiments with similar results.

(B) Left, RAW cells were treated with CO for the indicated times, and nuclear protein analyzed by Western blotting for PPARγ expression. Right, quantitative densitometric data expressed as PPARγ/TFIIB expression relative to untreated (air) control cells. Data are presented as mean (n = 3) ± SD ($p < 0.05$).

(C) RAW cells were transfected with the AOX -TK plasmid and exposed to CO (250 ppm) or ciglitazone as a positive control (10 μM) for 15 hr. Luciferase activity was normalized to total protein extract and expressed as a percentage of untreated (control) cells. Note that CO-evoked PPARγ reporter gene activation similar to ciglitazone. Data represent mean (n = 4) ± SD. Graph is representative of three independent experiments.

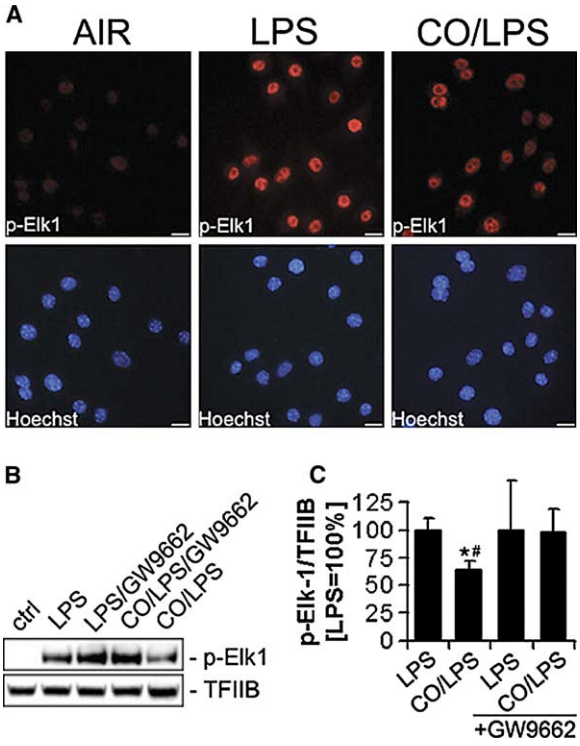

Figure 3. CO Inhibits Elk-1 Activation via PPARγ

(A) RAW cells LPS ± CO. Cells were fixed and stained for phospho-Elk1 expression. The image is representative of three experiments with similar results.

(B) RAW cells were treated with GW9662 ± CO. LPS was then added, and nuclear protein isolated and analyzed for phospho-Elk1 by Western blotting.

(C) Quantitative densitometric data are expressed as p-Elk-1/TFIIB expression relative to LPS-treated cells. Data represent mean (n = 3) ± SD (* and #, $p < 0.05$ versus LPS and CO/LPS/GW9662).

in nuclear Elk-1 phosphorylation. This increase was inhibited an average of 36% in the presence of CO (Figures 3A–3C). Inhibition of PPARγ by GW9662 did not affect LPS-induced nuclear Elk-1 phosphorylation; however, the inhibitory effect of CO on Elk-1 phosphorylation was reversed when PPARγ was inhibited (Figures 3B and 3C), consistent with a role for PPARγ in the CO effects rather than in the response to LPS.

CO Inhibits Expression of Egr-1-Dependent Procoagulant Genes In Vitro in a PPARγ-Dependent Manner

To extend our findings of the suppressive effect of CO and PPARγ on Egr-1 expression, we examined mRNA levels of tissue factor (TF) and plasminogen activator inhibitor-1 (PAI-1), two Egr-1-dependent genes that are involved in disseminated intravascular coagulation (Yan et al., 2000; Pawlinski et al., 2003). These assays were performed at times of peak Egr-1 protein expression/function (i.e., 60–240 min) (Figure 4A). The suppressive effects of CO on PAI-1 induced by hypoxia have previously been reported (Fujita et al., 2001), yet the cellular mechanisms by which this occurred were not elucidated. TF protein was undetectable regardless of the absence or presence of CO in resting macrophages (Figure 4B). Addition of LPS strongly increased TF expression, which was significantly suppressed (by 72.7%, 57.1%, and 51.9% after 5, 9, and 15 hr, respectively) (Figure 4B) in cells exposed to CO. To investigate the role of PPARγ in CO/LPS-modulated TF expression, we pretreated RAW cells with the selective PPARγ

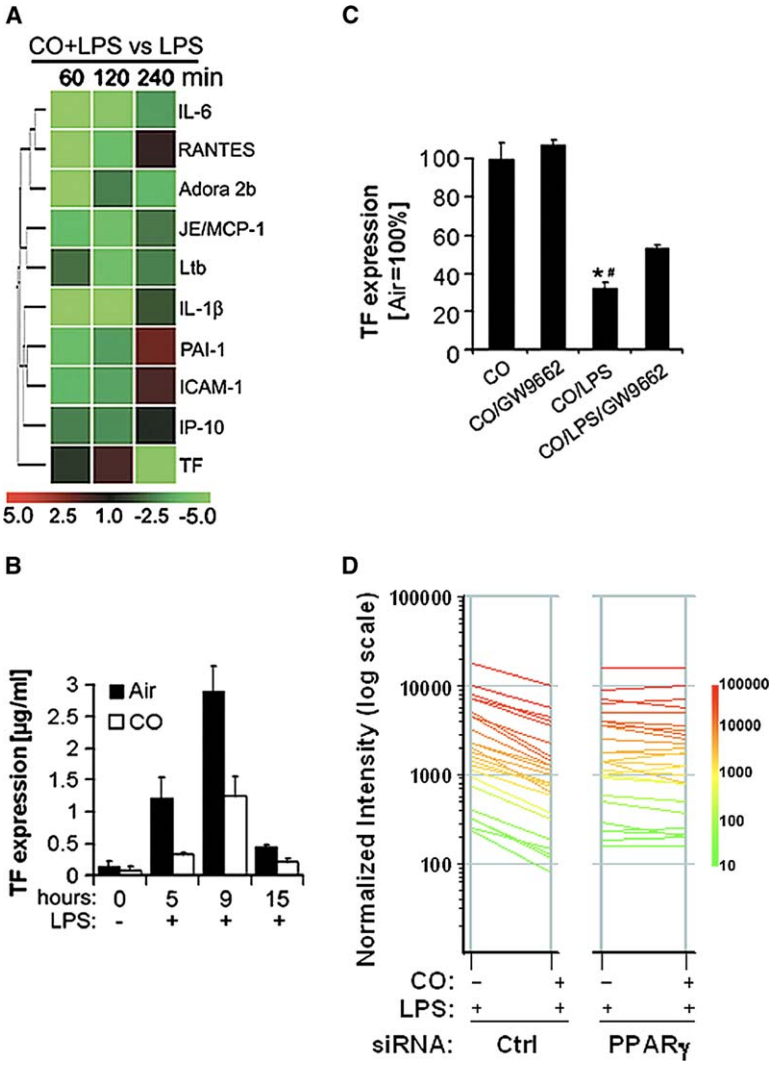

Figure 4. Suppression of Egr-1-Dependent Genes by CO: Role of PPARγ

(A and B) GeneChip data (see Supplemental Data) were examined for known Egr-1 responsive genes. Expression levels are expressed as ratio of CO + LPS versus LPS. The scale at the figure bottom denotes fold changes.

(B) TF protein expression of LPS-activated RAW 264.7 cells was determined with a two-stage clotting assay as described in the Experimental Procedures. Data represent mean (n = 4) ± SD ($p < 0.05$ versus LPS).

(C) RAW cells were treated with the PPARγ inhibitor GW9662 or vehicle (DMSO) ± CO (250 ppm). LPS was then added, and samples analyzed for TF expression. Results represent percent TF expression versus control (Air) samples. Data represent mean (n = 4) ± SD (* and #, $p < 0.05$ versus LPS and CO/LPS/GW9662).

(D) RNA profiling of ctrl-siRNA (left panel) or PPARγ siRNA (right panel) transfected RAW 264.7 cells with LPS (10 ng/ml) in the absence or presence of CO plotting 26 genes downregulated at least 2-fold in the ctrl-siRNA-treated cells that were subsequently reversed to control-LPS values in PPARγ-siRNA-treated cells. Genes are represented by colored lines according to their expression level. Results represent normalized mean fluorescence from duplicate experiments of each treatment group. A summary of significant differences are presented in Table S3. Complete GeneChip datasets are available online as GEO entry GSE1906: http://www.ncbi.nlm.nih.gov/projects/geo/.

inhibitor GW9662 prior to LPS or to CO/LPS. GW9662 did not affect LPS-induced TF expression in the absence of CO, whereas the CO-mediated suppression of TF expression was significantly reversed (Figure 4C). CO also suppressed LPS-induced PAI-1 protein expression (Figures S4A and S4B), and inhibition of PPARγ abrogated the CO-mediated suppression (Figure S4C). In order to explore whether these results were specific for a few genes (TF, Egr-1) or reflected a widespread requirement for PPARγ to mediate the anti-inflammatory effects of CO, we performed additional RNA profiling to analyze the ability of CO to inhibit gene expression in PPARγ-deficient cells. The results of duplicate microarray experiments performed on the Affymetrix platform, comparing mRNA extracted from control and PPARγ-siRNA transfected cells treated with LPS in the absence or presence of CO, are plotted in Figure 4D. For each treatment, all genes exhibiting an inhibition of more than 2-fold in the CO-treated ctrl-siRNA cells (left panel) were compared to their counterparts in CO-treated PPARγ-siRNA cells (right panel). This broader analysis revealed that CO-mediated inhibition was profoundly impaired in cells in which PPARγ was knocked down. Approximately 50% of the genes inhibited by CO in control siRNA treated cells were not inhibited in PPARγ-siRNA knocked down cells, including known PPARγ targets such as IL-6, IP-10, and thymidylate kinase family LPS-inducible member (Welch, et al., 2003) (Figure 4D and Table S3). Thus, PPARγ is broadly required for the anti-inflammatory mechanism of CO in LPS activated macrophages.

Effect of CO on LPS-Induced Lung Injury In Vivo

We assessed whether PPARγ modulates the protective effects of CO in vivo. We chose a lung injury model for our in vivo studies to evaluate the role of CO-induced PPARγ as the lung is a major target organ for LPS-induced inflammation. Additionally, we have shown previously that CO administered either pre- or post-LPS can limit neutrophil infiltration and tissue damage (Otterbein et al., 2003c; Sarady et al., 2004); however, the initiating mechanism and cellular targets by which CO had these effects remained unclear. Figure 5A shows that CO exposure (250 ppm, 6 hr) resulted in a significant expression of PPARγ selectively in alveolar macrophages. We conclude that macrophages are one of the key targets by which CO exerts its anti-inflammatory effects. Mice given LPS showed elevated Egr-1 protein levels

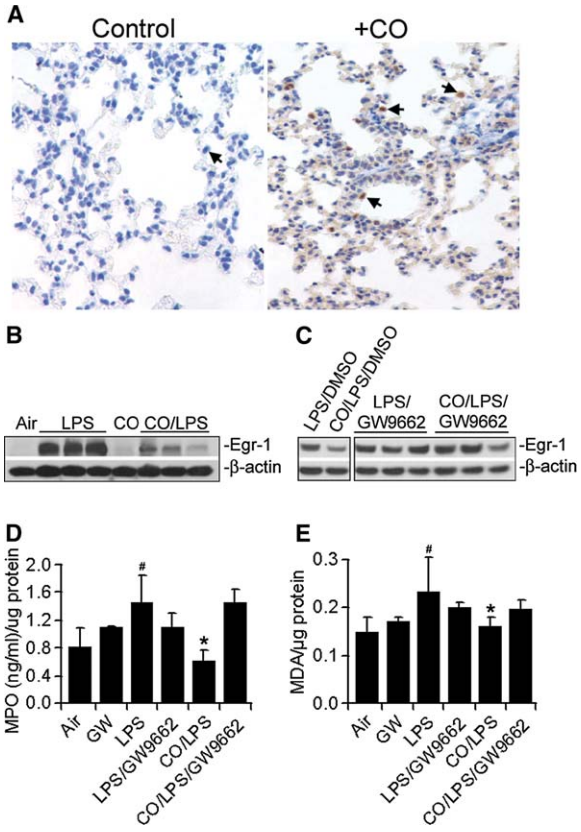

Figure 5. Effects of CO on Leukocyte Accumulation and Lung Damage in Endotoxin-Treated Mice Depends on PPARγ Activity

(A) Mice were exposed to CO for 6 hr. Lungs were harvested and immunostained for PPARγ protein expression (arrows indicate positive staining macrophages). Images are representative sections from 15–20 sections/lung from three to four individual mice/group. Bar represents 20 μm.

(B) Mice were exposed to CO for 1 hr followed by injection of LPS. Lungs were harvested, and Egr-1 protein expression was assessed by Western blot. β-actin demonstrates equal protein loading.

(C) Mice were pretreated with GW9662 (5 mg/kg, i.p.) for 1.5 hr prior to exposure to CO for 1 hr followed by injection of LPS. Lungs were harvested, and Egr-1 protein expression was assessed by Western blotting as in (B).

(D and E) Pulmonary neutrophil sequestration and tissue lipid peroxidation was measured by MPO and MDA accumulation, respectively. Mice were pretreated 30 min with GW9662 and then placed in CO or air prior to LPS. Sixteen hours later, the lungs were harvested and analyzed for MPO and MDA assessment. Data represent mean ± SD (six to eight mice/group). *$p < 0.01$ versus LPS, GW/LPS, and GW/CO/LPS; #$p = 0.02$ versus air.

in the lung as expected as well as leukocyte accumulation and lipid peroxidation (based on measurements of MPO and MDA accumulation, respectively, in lung extracts). PPARγ appeared not to be involved in these responses: administration of GW9662 did not affect Egr-1 expression or its proinflammatory consequences in response to LPS alone. CO significantly suppressed the LPS-mediated increase of Egr-1 (Figure 5B) as well as the increase in MPO and MDA in the lung (Figures 5D and 5E). We tested whether the CO effects in vivo required PPARγ by administrating GW9662 to mice 30 min prior to pretreatment with CO. Inhibition of PPARγ suppressed the anti-inflammatory effects of CO. These data indicate that CO led to a PPARγ-dependent anti-inflammatory response induced by LPS (Figures 5C–5E). Thus, the protective, anti-inflammatory effects of CO in the lung, as in macrophages in culture, rely on the ability of CO to increase expression of PPARγ that in turn prevents upregulation of Egr-1, a marker of the inflammatory response elicited by endotoxin.

CO Exposure Increases the Generation of Reactive Oxygen Species

Exposure of RAW 264.7 macrophages to CO resulted in a transient burst in DCF fluorescence indicative of production of reactive oxygen species (ROS) as early as 15 min and peaking at 60 min (Figure 6A). These effects were also observed in primary mouse alveolar macrophages (Figure 6A) and the human macrophage cell line THP-1 (data not shown). To identify the source of ROS in the cell, we depleted cells of mitochondria (Duranteau et al., 1998) and then exposed them to CO. As seen in Figure 6B, the ability of CO to generate ROS in mitochondria deficient cells (ρ^o) was markedly reduced versus that generated in wild-type cells. Furthermore, the CO-mediated increase in PPARγ expression was lost in mitochondria-deficient cells (Figure 6C). We propose that CO binds cytochrome oxidase, i.e., the heme-containing complex IV of the mitochondria (Alonso et al., 2003). The binding of CO to cytochrome oxidase at this concentration does not affect cellular respiration and ATP generation (data not shown). We tested the hypothesis that this increase in ROS by CO was involved in the upregulation of PPARγ by performing two sets of experiments. First, addition of the membrane-permeable antioxidants superoxide dismutase and catalase resulted in the loss of CO-induced ROS production and PPARγ expression (Figure 6D). Second, treatment of cells with Antimycin A, which selectively blocks mitochondrial electron transport at complex III, not only effectively abrogated CO-induced ROS and PPARγ expression (Figure 6D) but also reversed the inhibitory effect of CO on LPS-induced Egr-1 expression (Figure 6E). We saw similar effects if cells were treated with the alternative complex III inhibitor myxothiazol (data not shown). We conclude that blocking electron transport at complex III prevents electrons from being transferred to complex IV to increase superoxide generation. Moreover, by providing the antioxidant enzymes, superoxide anion and hydrogen peroxide are rapidly removed and therefore cannot contribute to mediating the CO response. These data suggest that the mitochondria are at least one of the targets for CO in macrophages and that the burst of ROS leads to the subsequent activation of PPARγ.

Discussion

The most significant findings of the present study are the demonstration that CO alone leads to the generation of mitochondrial ROS that, in turn, play a role as signaling molecules to upregulate PPARγ, and further, that PPARγ, at least in large measure, accounts for the anti-inflammatory effects of CO in vitro and in vivo. By upregulating PPARγ, CO by itself alters the molecular response machinery of the cell such that a subsequent stress stimulus, in this case endotoxin, generates an anti-inflammatory as opposed to the classical

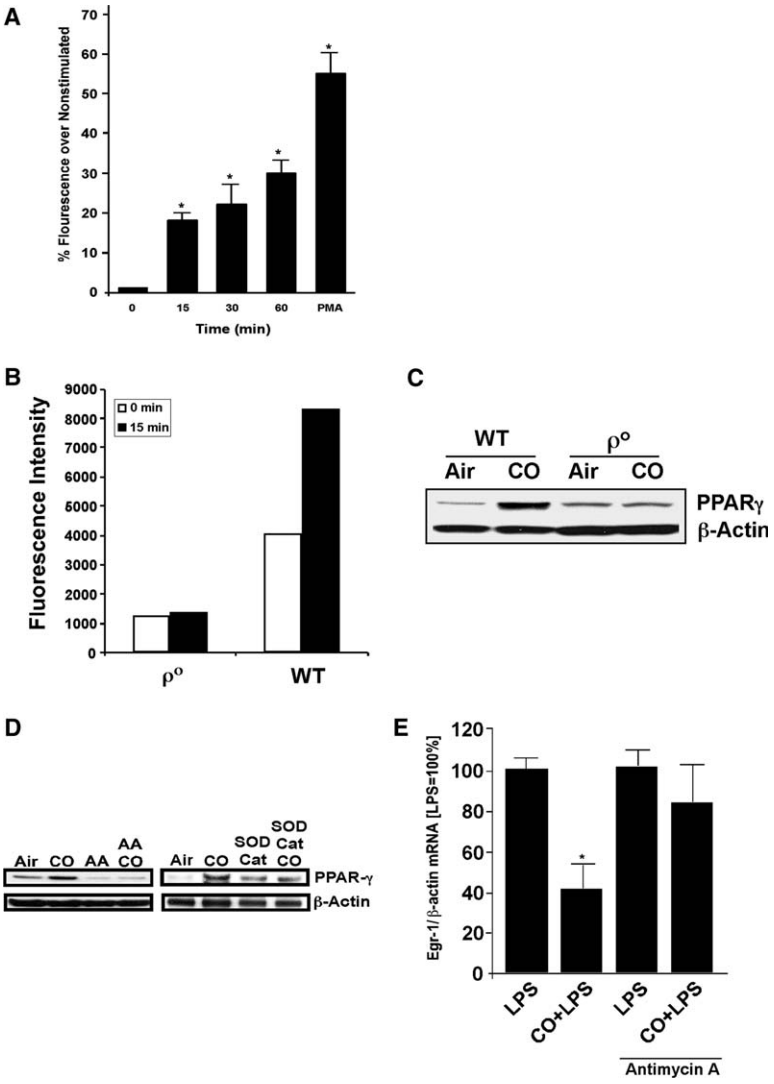

Figure 6. CO Exposure Increases ROS Generation that Is Responsible for CO-Induced PPARγ Upregulation

(A) Kinetics of CO-induced increases in DCF fluorescence. RAW 264.7 cells were exposed to CO after addition of DCFH-DA. Relative flouresence was compared to DCFH-DA-loaded air-treated cells. PMA was used as a positive assay control.

(B) Mitochondrial-deficient cells (ρ^o) do not generate ROS in response to CO. Results represent mean ± SD of four measurements at each time point from three separate experiments.

(C) Wild-type (wt) or mitochondrial-deficient cells (ρ^o) were treated with CO (250 ppm) for 4 hr, and PPARγ expression was determined thereafter. The blot is a representative image from three separate experiments.

(D) RAW 264.7 cells were pretreated with either antimycin A or PEG-SOD + PEG-catalase prior to CO. Expression of PPARγ was determined 4 hr later. Note that interference with electron transport as well as the presence of the antioxidant enzymes prevented the ability of CO to upregulate PPARγ. Blots are representative images from three separate experiments.

(E) RAW 264.7 cells were pretreated with antimycin A prior to CO. LPS was then added, and Egr-1 mRNA expression analyzed by RT-PCR. Note that interference with electron transport prevented the ability of CO to inhibit LPS-induced Egr-1 expression. Data are mean (n = 3) ± SD (*p < 0.05 versus LPS and CO + LPS + antimycin A).

proinflammatory response. CO exposure has been shown to induce a number of other molecules, including NF-κB in hepatocytes (Zuckerbraun et al., 2003) and cGMP in smooth muscle cells (Morita et al., 1997; Peyton et al., 2002; Otterbein et al., 2003b). To what extent these other molecules have a similar role in the benefits afforded by CO remains to be elucidated. A recent report by Reinking et al. describes a heme-containing nuclear receptor that is responsive to gases including NO and CO in *Drosophila*. They go on to suggest that this receptor may function as a gas sensor that mediates intracellular signaling (Reinking et al., 2005). A similar report by Dioum et al. describes a gas-responsive PAS2 domain transcription factor in the murine nervous system (Dioum et al., 2002). Whether such a factor exists in other cell types remains to be determined. The identification of gas-specific CO-responsive molecules supports our findings of a role for CO as a homeostatic molecule and emphasizes the overall importance of CO and other gases such as nitric oxide as biological effectors in the inflammatory system.

We focused on Egr-1, a key transcription factor for the generation of the inflammatory response in macrophages (Guha et al., 2001; Yan et al., 2000). Egr-1 mRNA, protein, and activity were rapidly induced by LPS both in vitro and in vivo in the lung. Pretreatment with CO resulted in almost complete suppression of Egr-1 mRNA and protein expression as well as DNA binding activity (Figure 1). These suppressive effects of CO on Egr-1 (as well as the corresponding suppression of TF and PAI-1) were PPARγ dependent: the upregulation of PPARγ by CO (Figure 2) was essential for the suppression of Egr-1 by CO. Both in the in vitro and in vivo models, the protective effect was lost with PPARγ inhibition either pharmacologically or genetically. These results reveal an important molecular target for CO.

The inhibitory effect of CO on Egr-1 expression and function in RAW cells resulted in a decrease in mRNA and protein expression of Egr-1 target genes, including TF (Figure 4). The critical effect of Egr-1 on TF expression has been shown in LPS-stimulated *egr-1*$^{-/-}$ mice in which TF upregulation was virtually absent (Pawlinski et al., 2003). We hypothesized that inhibition of Egr-1 activity by PPARγ could be the mechanism by which CO exerts its repressive effect on TF transcription. Indeed,

inhibition of PPARγ partially restored LPS-induced TF expression in cells exposed to CO.

A major goal in the current studies was to identify an early cellular event (or events) stimulated by CO alone that could explain the suppressive effects of CO on the LPS response. Our gene chip analysis identified Egr-1 as being highly upregulated by LPS and just as significantly downregulated by CO pretreatment before LPS. It was known that PPARγ potently regulates Egr-1 (Okada et al., 2002). Additionally, the effects of PPARγ are very similar to those of CO when examined in identical models, i.e., both have anti-inflammatory and antiproliferative effects (Chawla et al., 2001; Otterbein et al., 2003a; Okada et al., 2002; Simonin et al., 2002; Jiang et al., 1998; Theocharis et al., 2004). This supported our hypothesis that CO might function in part via PPARγ. The data presented here show that PPARγ is upregulated in macrophages in vitro and in vivo before the addition of LPS, presumably conditioning the cells to respond in an anti-inflammatory fashion to protect the cell and limit lung leukocyte infiltration and tissue damage. We speculate that similar mechanisms are operative in other inflammatory models, such as hyperoxia and ischemia/reperfusion-induced lung injury, where CO has been shown to be protective (Zhang et al., 2003; Otterbein et al., 2003a; Fujita et al., 2001; Song et al., 2003).

Since CO is most likely to bind to a hemoprotein, it is unlikely that PPARγ, which does not contain a heme moiety, is the initial molecular contact for CO. While searching for a molecular target that might be involved upstream of PPARγ, we noted that CO rapidly stimulates a transient and relatively low intensity oxidative burst originating from the mitochondria. The resultant ROS are involved in the subsequent induction of PPARγ. To assess whether CO might increase expression of PPARγ ligands and thus regulate PPARγ activation, we transiently cotransfected a chimeric fusion plasmid containing the PPARγ ligand binding domain (LBD) fused to the Gal4 DNA binding domain (pCMV-Gal4-PPARγ LBD) and a reporter plasmid containing the luciferase gene under regulation by four Gal4 DNA binding elements (pFR-Luc; kind gifts from J. Flier, Department of Endocrinology, Beth Israel Deaconess Medical Center, Boston, MA) (Schopfer et al., 2004). Exposure to known ligands such as troglitazone resulted in the expected increase in luciferase (>7-fold) as expected, while no change in luciferase was observed in cells exposed to CO (data now shown). We conclude from these experiments that increased ligand generation is not a mechanism by which CO modulates PPARγ expression and activity. The upregulation of PPARγ by the oxidative burst occurs very quickly in response to CO. We see increases in ROS generation as early as 5 min of exposure (data not shown). Whether other mechanisms exist that would also explain how CO facilitates accumulation of PPARγ and thus suppresses Egr-1 remains to be elucidated. Nuclear-cytoplasmic shuttling of PPARγ as well as modulation of the proteasome pathway (which regulates PPARγ function) may also be involved (Cheng et al., 2004; Kelly et al., 2004).

There is accumulating evidence of a role for PPARγ in the regulation of pro- and anti-inflammatory transcription factors, including Egr-1, NF-κB, SP-1, and NF-AT (Shi et al., 2002; Yang et al., 2000; Cheng et al., 2004; Kelly et al., 2004). Consistent with our finding that the inhibitory effects of CO on LPS-induced Egr-1 expression are acting via PPARγ activation is our observation that inhibition of PPARγ reversed the CO-inhibitory effect on activation of Elk-1, which mediates Egr-1 gene expression (Shi et al., 2002; Okada et al., 2002). There are previous reports on the relationship of PPARγ to Elk-1 and Egr-1 (Guha et al., 2001). Overexpression of wild-type PPARγ in human synovial fibroblasts suppressed transcriptional activity of a luciferase reporter construct containing putative Egr-1 binding sites (Sugawara et al., 2002); the inhibition of luciferase activity was further enhanced in the presence of the PPARγ agonist $15dPGJ_2$ (Sugawara et al., 2002). PPARγ ligands were also reported to inhibit hypoxia-induced Egr-1 expression in mononuclear phagocytes (Okada et al., 2002).

CO may also suppress Egr-1 by mechanisms independent of PPARγ as reversal by the selective inhibitor is not complete. Theoretical possibilities include involvement of the ERK-1/2 MAPK pathway, cGMP or NAB2, which is an inducible corepressor of Egr-1 (Shi et al., 2002; Fujita et al., 2001; Chen et al., 2003; Lucerna et al., 2003). However, CO does not modulate ERK-1/2 activation or increases in cGMP in RAW cells (Otterbein et al., 2000), arguing against the possibility that CO inhibits Egr-1 expression via blockade of ERK-1/2. Likewise, NAB2 mRNA levels in LPS- and CO/LPS-treated RAW macrophages were similar (data not shown), making it less likely that CO acts through NAB2. We have previously documented the involvement of p38 MAPK in CO-mediated suppression of vascular smooth muscle cell proliferation as well as the ability of CO to block LPS-induced NF-κB activation in the lung (Sarady et al., 2004). Neither of these effects has to date been linked to PPARγ. The role of p38 MAPK and the augmented activation state of p38 MAPK induced by CO as well as the decreased activity of NF-κB manifest themselves only after pretreatment with CO followed by stimulation with LPS in this model; both are either weakly or not affected by CO alone during the pretreatment period (Otterbein et al., 2000; Fujita et al., 2001). Further studies will be needed to evaluate whether CO-induced PPARγ is involved in the previously reported effects of CO pretreatment on the response to LPS of p38 MAPK and/or NF-κB (Otterbein et al., 2000; Sarady et al., 2004). For the moment, we conclude that PPARγ suppresses LPS-induced Egr-1 expression by inhibiting Elk-1 activation, leaving open the possibility that this may involve effects on p38 and NF-κB.

How the ROS burst in response to CO leads to PPARγ upregulation is unknown. The reports from Reinking and Dioum mentioned above make clear that there are alternative hemoproteins that might also be involved in the cellular response to CO or perhaps integrated into the PPARγ effects. We speculate that either a ROS-sensitive intermediate is involved or that PPARγ itself is directly regulated by the oxidative burst. Potential targets for the CO-induced ROS might include modulation of the protein phosphatases, decreased degradation of PPARγ (Hauser et al., 2000), or differential regulation of scaffold regulatory corepressor or coactivator proteins such as PGC-1, nuclear hormone receptor corepressor (NcoR), and silencing mediator for retinoid and

thyroid hormone receptors (SMRT), phosphorylation by MAP kinases (Gelman et al., 2005), or SUMOylation (Pascual et al., 2005). These results give support to our model that CO at low concentrations orchestrates the molecular machinery of the cell in a manner that will determine the subsequent response to stress.

Experimental Procedures

Cell Culture

RAW 264.7 mouse peritoneal macrophages from ATCC (Rockville, MD) and primary mouse alveolar macrophages obtained via bronchoalveolar lavage of C57BL/6 mice were cultured in DMEM containing 10% FBS and 100 μg/ml gentamicin. Cells were exposed to 2–4 hr CO (250 ppm) or air as previously described (Otterbein et al., 2000) prior to addition of LPS (1 ng/ml *E. coli* serotype O127:B8; Sigma, St. Louis, MO). GW9662 was purchased from Calbiochem (San Diego, CA). Antimycin A, PEG-Catalase, and PEG-SOD were purchased from Sigma Chemical (St. Louis, MO). All agents were used at the indicated concentrations.

Semiquantitative RT-PCR

Using the software Primer3 (Whitehead Institute/MIT Center for Genome Research; http://www.genome.wi.mit.edu/), we selected sequence-specific primers from the full-length published cDNA sequences (Table S1). Two hundred nanograms total RNA was amplified with the One-Step RT-PCR kit (Qiagen). Reverse transcription was carried out at 55ºC for 30 min, and HotStarTaq DNA polymerase was activated at 95ºC for 15 min followed by 24–27 cycles of amplification (94ºC for 30 s, 55ºC for 30 s, and 72ºC for 60 s) and final extension at 72ºC for 10 min. Amplified PCR products were separated by agarose gel electrophoresis and stained with ethidium bromide.

Real-Time PCR

Total RNA (1 μg) was reverse transcribed into cDNA by MMLV enzyme (Promega, Mannheim, Germany) with random heaxamers (1 μg/μg total RNA). The reaction mixture was incubated at 37ºC for 45 min followed by 15 min at 45ºC and 20 min at 70ºC. All PCRs were performed with the SYBR Green kit (BioRad, Hercules, CA). Primers for selected genes are listed in Table S1. By using a Mx3000P QPCR System (Stratagene, La Jolla, CA), PCR cycling conditions were as follows: initial denaturation at 95ºC for 10 min, followed by 40 cycles at 94ºC for 30 s, 58ºC for 15 s, and 72ºC for 30 s and a 10 min terminal incubation at 72ºC. Sequence Detector Software (Stratagene) was used to extract the PCR data, which were then exported to Excel (Microsoft, Redmond, WA) for further analysis. Expression of target genes was normalized to β-actin expression levels.

SDS-PAGE and Western Blotting

Cells and tissue lysates were separated by SDS-PAGE and blotted as described previously (Otterbein et al., 2000; Fujita et al., 2001). Blots were incubated with primary rabbit anti-Egr-1, mouse anti-phospho-Elk-1 (Santa Cruz Biotechnology, Santa Cruz, CA), or rabbit anti-PPARγ (Upstate, Lake Placid, NY). Membranes were then washed in TTBS and visualized with HRP-conjugated antibody against rabbit or mouse IgG and the ECL reagents (Amersham, Piscataway, NJ) per manufacturer's instructions. To confirm equal loading, we reprobed blots with mouse monoclonal antibody targeting β-actin (Abcam, Inc., Cambridge, MA) or rabbit anti-TFIIB IgG.

Transfection and Transient Reporter Assays

RAW 264.7 cells were transfected in the presence of 10% FCS at 1 μg/well with the PPAR-responsive reporter plasmid p(AOX)3-TKSL (kindly provided by C.K. Glass; Department of Medicine, University of California, San Diego, La Jolla, CA) with Lipofectamine 2000 (according to the manufacturer's instructions; Invitrogen, Carlsbad, CA). Six hours later, cells were washed and treated with CO or ciglitazone (BioMol, Plymouth Meeting, PA). After 15 hr, protein extracts were assessed for luciferase activity (Promega, Madison, WI). Luminescence values were normalized to total protein levels and presented as the percentage of luciferase activity measured with CO or troglitizone or rosiglitazone.

PPARγ-Knockdown Assays

RAW 264.7 cells were plated in 12-well plates at a density of 1.5×10^5 cells/well. On the next day, the cells were transfected with 100 nM PPARγ-SMARTpool reagent (Dharmacon) with Lipofectamine 2000. Four siRNA sequences were tested of which one was used for experimentation (#2; see Figure S1 for sequence and method). For PPARγ knockdown assays, the preannealed oligo (Dharmacon; 5′-GAC AUG AAU UCC UUA AUG AUU -3′; bp 874–893 of GenBank NM_011146) was used at 100 nM. The medium was replaced 36 hr later, and cells were stimulated with LPS another 12 hr later in the absence or presence of CO. RT-PCR was employed to assess Egr-1 and β-actin mRNA levels. A GC-control oligo (catalog number, D-001206-01-05; target sequence, 5′-NNATGAACGTGAATTGCTCAA-3′; Dharmacon) was used at the same concentration.

DCF Fluorescence as a Measure of Intracellular Production of ROS

RAW 264.7 macrophages were incubated with air or CO (250 ppm) for 5–60 min. Cells were loaded with DCFH-DA (Molecular Probes, Eugene, OR; 5 μM) 15 min prior to harvest time point. Cells were then washed and resuspended in FACS buffer (PBS + 1% FBS), and fluorescence was measured as previously described (Duranteau et al., 1998).

Generation of Mitochondrial-Deficient ρ^o Cells

RAW 264.7 cells were grown as above and supplemented with 50 ng/ml ethidium bromide (EtBr), 100 μg/ml pyruvate, and 50 μg/ml uridine. EtBr treatment was suspended after 14 doubling times (~21 days). Cells were then tested for their ability to survive "ρ^o selection media" consisting of DMEM/10% FBS plus pyruvate and pyrimidines that confirmed auxotrophy. Surviving colonies were subcultured in ρ^o selection media.

Immunostaining

Cells grown on coverslips were washed, fixed with 4% paraformaldehyde, permeabilized with Triton-X 100, and blocked with goat serum. Expression of PPARγ and p-Elk-1 were detected with antibodies described above and visualized with Alexa-594 conjugated goat anti-mouse or goat anti-rabbit antibodies (Molecular Probes). Nuclei were visualized with Hoechst 33258 (Sigma). Pictures were captured with a Zeiss Axio Microscope (Carl Zeiss Optics, Jena, Germany). PPARγ was detected in frozen lung sections with rabbit anti-PPARγ polyclonal Ab (Upstate, Inc., Waltham, MA). Eight to ten images from each animal were captured.

Electrophoretic Mobility Shift Assays

Nuclear extracts were prepared according to a modified Shapiro's method (Shapiro et al., 1988). Gel-purified oligonucleotides (Oligos Etc., Wilsonville, OR) containing the consensus binding site for Egr-1 (5′-GGATCCAGCGGGGGCGAGCGGGGGCGA-3′ and 3′-CCTAGGTCGCCCCCGCTCGCCCCCGCT-5′) were labeled with 32P ATP and used for EMSA. Electrophoresis mobility shift assays (EMSA) reactions were assembled and run as described previously (Usheva and Shenk, 1996).

Measurement of Tissue Factor Activity

Tissue factory (TF) activity was measured with a two-stage chromogenic reaction as described previously (Kopp et al., 1998).

Adenoviral Infections of Bone-Marrow-Derived Macrophages

Bone-marrow-derived macrophages (BMDM) were isolated from B6.129-Pparg$^{tm2Rev/J}$ mice (Jackson Laboratory, Bar Harbor, ME) and differentiated as previously described (Xiong et al., 2004).

Recombinant adenoviral stocks were obtained from the Gene Transfer Vector Core facility at the University of Iowa College of Medicine (Iowa City, IA). Infections (*Cre* recombinase and control virus) were performed with a concentration of 25 MOI/cell. Infections were performed on day 4 post harvest as previously described (Brouard et al., 2000). All experiments were performed on day 5–6. To assess *Cre* activities in transduced PPARγ lox-BMDMs, total RNA was extracted 3 days posttransduction and subjected to

semiquantitative RT-PCR as described (Hevener et al., 2003). Two oligonucleotides located in exons A1 and A4 of the PPARγ1 gene were designed to recognize the full length (700 bp) and recombined messages (300 bp): GTCACGTTCTGACAGGACTGTGTGAC (5′-) and TATCACTGGAGATCTCCGCCAACAGC (3′-).

Endotoxin-Induced Acute Lung Injury in Mice

Male C57BL/6J mice from Jackson labs were housed at the University of Pittsburgh or Beth Israel Deaconess Medical Center Animal Facilities and allowed to acclimate 1 week prior to experimentation. The protocol was approved by the University of Pittsburgh and Beth Israel Deaconess Medical Center Animal Care and Use Committees. On the day of experimentation, mice were treated with GW6996 (5 mg/kg, i.p.) 30 min prior to being placed in CO (250 ppm) (Otterbein et al., 2000) or maintained in room air. One hour thereafter, the mice were administered LPS (1 mg/kg, i.p.) and returned to room air for the duration of the experiment. Sixteen hours post LPS, the animals were sacrificed, and the lungs harvested and snap frozen in liquid N_2. Lung tissue was divided and processed for protein determination and measurements of malondialdehyde (MDA) and myeloperoxidase (MPO) with kits per manufacturer's instructions (R&D, Minneapolis, MN, and Oxidoresearch, Portland, OR, respectively). Results are expressed per mg total protein to normalize.

Statistical Analysis

Band intensities were quantified by densitometric analyses with a MultiImage Densitometer and ChemiImage 5500 software (Alpha Innotech, San Leandro, CA). Statistical analysis was made by using Student's t test. Results were considered statistically significant at $p < 0.05$.

Supplemental Data

Supplemental Data include the method for cRNA synthesis and gene expression profiling as well as additional supporting figures and tables referenced within the text. These are available at http://www.immunity.com/cgi/content/full/24/5/601/DC1/.

Acknowledgments

We thank Eva Muzik for assistance with GeneChip experiments and David Gallo for assistance with animal experiments. This work was supported by National Institutes of Health grants HL-071797 and HL-076167 (L.E.O.) and HL-58688 (F.H.B.) and Atorvastatin Research Award (AHA) sponsored by Pfizer (awarded to L.E.O.) and grant 10239 Jubilee Fund, Austrian National Bank, Vienna (to M.B.). This work was also supported by the Transplant Center and the Julie Henry Fund at the Beth Israel Deaconess Medical Center. L.E.O. is a paid consultant of Linde Gas Therapeutics.

Received: May 18, 2005
Revised: January 16, 2006
Accepted: March 10, 2006
Published: May 23, 2006

References

Alonso, J., Cardellach, F., Lopez, S., Casademont, J., and Miro, O. (2003). Carbon monoxide specifically inhibits cytochrome c oxidase of human mitochondrial respiratory chain. Pharmacol. Toxicol. *93*, 142–146.

Brouard, S., Otterbein, L.E., Arather, J., Tobiasch, E., Bach, F.H., Choi, A.M., and Soares, M.P. (2000). Carbon monoxide generated by heme oxygenase 1 suppresses endothelial cell apoptosis. J. Exp. Med. *192*, 1015–1026.

Chawla, A., Barak, Y., Nagy, L., Liao, D., Tontonoz, P., and Evans, R. (2001). PPAR-gamma dependent and independent effects on macrophage-gene expression in lipid metabolism and inflammation. Nat. Med. *7*, 48–52.

Chen, F., Wang, M., O'Connor, J., He, M., Tripathi, T., and Harrison, L.E. (2003). Phosphorylation of PPARgamma via active ERK1/2 leads to its physical association with p65 and inhibition of NF-kappabeta. J. Cell. Biochem. *90*, 732–744.

Cheng, S., Afif, H., Martel-Pelletier, J., Pelletier, J., Li, X., Farrajota, K., Lavigne, M., and Fahmi, H. (2004). Activation of human T lymphocytes is inhibited by peroxisome proliferator-activated receptor gamma (PPARgamma) agonists. PPARgamma co-association with transcription factor NFAT. J. Biol. Chem. *279*, 22057–22065.

Delerive, P., Fruchart, J.C., and Staels, B. (2001). Peroxisome proliferator-activated receptors in inflammation control. J. Endocrinol. *169*, 453–459.

Dioum, E.M., Rutter, J., Tuckerman, J.R., Gonzalez, G., Gilles-Gonzalez, M.A., and McKnight, S.L. (2002). NPAS2: a gas-responsive transcription factor. Science *298*, 2385–2387.

Duranteau, J., Chandel, N., Shao, Z., and Schumacker, P. (1998). Intracellular signaling by reactive oxygen species during hypoxia in cardiomyocytes. J. Biol. Chem. *273*, 11619–11625.

Fujita, T., Toda, K., Karimova, A., Yan, S., Naka, Y., Yet, S., and Pinsky, D. (2001). Paradoxical rescue from ischemic lung injury by inhaled carbon monoxide driven by derepression of fibrinolysis. Nat. Med. *7*, 598–604.

Gelman, L., Michalik, L., Desvergne, B., and Wahli, W. (2005). Kinase signaling cascades that modulate peroxisome proliferator-activated receptors. Curr. Opin. Cell Biol. *17*, 216–222.

Guha, M., O'Connell, M., Pawlinski, R., Hollis, A., McGovern, P., Yan, S., Stern, D., and Mackman, N. (2001). Lipopolysaccharide activation of the MEK-ERK1/2 pathway in human monocytic cells mediates tissue factor and tumor necrosis factor alpha expression by inducing Elk-1 phosphorylation and Egr-1 expression. Blood *98*, 1429–1439.

Hauser, S., Adelmant, G., Sarraf, P., Wright, H.M., Mueller, E., and Spiegelman, B.M. (2000). Degradation of the peroxisome proliferator-activated receptor gamma is linked to ligand-dependent activation. J. Biol. Chem. *275*, 18527–18533.

Hevener, A.L., He, W., Barak, Y., Le, J., Bandyopadhyay, G., Olson, P., Wilkes, J., Evans, R.M., and Olefsky, J. (2003). Muscle-specific Pparg deletion causes insulin resistance. Nat. Med. *9*, 1491–1497.

Jiang, C., Ting, A., and Seed, B. (1998). PPAR-gamma agonists inhibit production of monocyte inflammatory cytokines. Nature *391*, 82–86.

Kelly, D., Campbell, J., King, T., Grant, G., Jansson, E., Coutts, A., Pettersson, S., and Conway, S. (2004). Commensal anaerobic gut bacteria attenuate inflammation by regulating nuclear-cytoplasmic shuttling of PPAR-gamma and RelA. Nat. Immunol. *5*, 104–112.

Kopp, C., Robson, S., Siegel, J., Anrather, J., Winkler, H., Grey, S., Kaczmarek, E., Bach, F., and Geczy, C. (1998). Regulation of monocyte tissue factor activity by allogeneic and xenogeneic endothelial cells. Thromb. Haemost. *79*, 529–538.

Lucerna, M., Mechtcheriakova, D., Kadl, A., Schabbauer, G., Schafer, R., Gruber, F., Koshelnick, Y., Muller, H.D., Issbrucker, K., Clauss, M., et al. (2003). NAB2, a corepressor of EGR-1, inhibits vascular endothelial growth factor-mediated gene induction and angiogenic responses of endothelial cells. J. Biol. Chem. *278*, 11433–11440.

Morita, T., Mitsialis, S.A., Koike, H., Liu, Y., and Kourembanas, S. (1997). Carbon monoxide controls the proliferation of hypoxic vascular smooth muscle cells. J. Biol. Chem. *272*, 32804–32809.

Okada, M., Yan, S., and Pinsky, D. (2002). Peroxisome proliferator-activated receptor-gamma (PPAR-gamma) activation suppresses ischemic induction of Egr-1 and its inflammatory gene targets. FASEB J. *16*, 1861–1868.

Otterbein, L., Bach, F., Alam, J., Soares, M., Tao Lu, H., Wysk, M., Davis, R.J., Flavell, R.A., and Choi, A.M. (2000). Carbon monoxide has anti-inflammatory effects involving the mitogen-activated protein kinase pathway. Nat. Med. *6*, 422–428.

Otterbein, L.E., Soares, M.P., Yamashita, K., and Bach, F. (2003a). Heme oxygenase-1: unleashing the protective properties of heme. Trends Immunol. *24*, 449–455.

Otterbein, L.E., Otterbein, S.L., Ifedigbo, E., Liu, F., Morse, D., Fearns, C., Ulevitch, R., Knickelbein, R., Flavell, R., and Choi, A. (2003b). MKK3 mitogen-activated protein kinase pathway mediates carbon monoxide-induced protection against oxidant-induced lung injury. Am. J. Pathol. *163*, 2555–2563.

Otterbein, L., Zuckerbraun, B., Haga, M., Liu, F., Song, R., Usheva, A., Stachulak, C., Bodyak, N., Smith, R., Csizmadia, E., et al. (2003c). Carbon monoxide suppresses arteriosclerotic lesions associated with chronic graft rejection and with balloon injury. Nat. Med. *9*, 183–190.

Pascual, G., Fong, A.L., Ogawa, S., Gamliel, A., Li, A.C., Perissi, V., Rose, D.W., Willson, T.M., Rosenfeld, M.G., and Glass, C.K. (2005). A SUMOylation-dependent pathway mediates transrepression of inflammatory response genes by PPAR-gamma. Nature *437*, 759–763.

Pawlinski, R., Pedersen, B., Kehrle, B., Aird, W., Frank, R., Guha, M., and Mackman, N. (2003). Regulation of tissue factor and inflammatory mediators by Egr-1 in a mouse endotoxemia model. Blood *101*, 3940–3947.

Peyton, K.J., Reyna, S.V., Chapman, G.B., Ensenat, D., Liu, X.M., Wang, H., Schafer, A.I., and Durante, W. (2002). Heme oxygenase-1-derived carbon monoxide is an autocrine inhibitor of vascular smooth muscle cell growth. Blood *99*, 4443–4448.

Reinking, J., Lam, M.M., Pardee, K., Sampson, H.M., Liu, S., Yang, P., Williams, S., White, W., Lajoie, G., Edwards, A., and Krause, H.M. (2005). The *Drosophila* nuclear receptor e75 contains heme and is gas responsive. Cell *122*, 195–207.

Ricote, M., Li, A.C., Willson, T.M., Kelly, C.J., and Glass, C.K. (1998). The peroxisome proliferator-activated receptor-gamma is a negative regulator of macrophage activation. Nature *391*, 79–82.

Sarady, J., Zuckerbraun, B., Bilban, M., Liu, F., Zamora, R., Choi, A., and Otterbein, L.E. (2004). Carbon monoxide protection against endotoxic shock involves reciprocal effects on iNOS in the lung and liver. FASEB J. *18*, 854–856.

Schopfer, F.J., Lin, Y., Baker, P.R., Cui, T., Garcia-Barrio, M., Zhang, J., Chen, K., Chen, Y.E., and Freeman, B.A. (2004). Nitrolinoleic acid: an endogenous peroxisome proliferator-activated receptor gamma ligand. Proc. Natl. Acad. Sci. USA *102*, 2340–2345.

Shapiro, D.J., Sharp, P.A., Wahli, W.W., and Keller, M.J. (1988). A high-efficiency HeLa cell nuclear transcription extract. DNA *7*, 47–55.

Shi, L., Kishore, R., McMullen, M., and Nagy, L. (2002). Lipopolysaccharide stimulation of ERK1/2 increases TNF-alpha production via Egr-1. Am. J. Physiol. Cell Physiol. *282*, C1205–C1211.

Simonin, M., Bordji, K., Boyault, S., Bianchi, A., Gouze, E., Becuwe, P., Dauca, M., Netter, P., and Terlain, B. (2002). PPAR-gamma ligands modulate effects of LPS in stimulated rat synovial fibroblasts. Am. J. Physiol. Cell Physiol. *282*, C125–C133.

Sugawara, A., Uruno, A., Kudo, M., Ikeda, Y., Sato, K., Taniyama, Y., Ito, S., and Takeuchi, K. (2002). Transcription suppression of thromboxane receptor gene by peroxisome proliferator-activated receptor-gamma via an interaction with Sp1 in vascular smooth muscle cells. J. Biol. Chem. *277*, 9676–9683.

Song, R., Kubo, M., Morse, D., Zhou, Z., Zhang, X., Dauber, J.H., Fabisiak, J., Alber, S.M., Watkins, S.C., Zuckerbraun, B.S., et al. (2003). Carbon monoxide induces cytoprotection in rat orthotopic lung transplantation via anti-inflammatory and anti-apoptotic effects. Am. J. Pathol. *163*, 231–242.

Theocharis, S., Margeli, A., Vielh, P., and Kouraklis, G. (2004). Peroxisome proliferator-activated receptor-gamma ligands as cell-cycle modulators. Cancer Treat. Rev. *30*, 545–554.

Usheva, A., and Shenk, T. (1996). YY1 transcriptional initiator: protein interactions and association with a DNA site containing unpaired strands. Proc. Natl. Acad. Sci. U.S.A. *93*, 13571–13576.

Welch, J.S., Ricote, M., Akiyama, T.E., Gonzalez, F.J., and Glass, C.K. (2003). PPARgamma and PPARdelta negatively regulate specific subsets of lipopolysaccharide and IFN-gamma target genes in macrophages. Proc. Natl. Acad. Sci. USA *100*, 6712–6717.

Xiong, H., Zhu, C., Li, F., Hegazi, R., He, K., Babyatsky, M., Bauer, A.J., and Plevy, S.E. (2004). Inhibition of interleukin-12 p40 transcription and NF-kappaB activation by nitric oxide in murine macrophages and dendritic cells. J. Biol. Chem. *279*, 10776–10783.

Yan, S., Fujita, T., Lu, J., Okada, K., Shan Zou, Y., Mackman, N., Pinsky, D., and Stern, D. (2000). Lipopolysaccharide activation of the MEK-ERK1/2 pathway in human monocytic cells mediates tissue factor and tumor necrosis factor alpha expression by inducing Elk-1 phosphorylation and Egr-1 expression. Nat. Med. *6*, 1355–1361.

Yang, X., Wang, L., Chen, T., Resau, J., DaSilva, L., and Farrar, W. (2000). Activation of human T lymphocytes is inhibited by peroxisome proliferator-activated receptor gamma (PPARgamma) agonists. PPARgamma co-association with transcription factor NFAT J. Biol. Chem. *275*, 4541–4544.

Zhang, X., Shan, P., Otterbein, L., Alam, J., Flavell, R., Davis, R., Choi, A., and Lee, P. (2003). Carbon monoxide modulates Fas/Fas ligand, caspases, and Bcl-2 family proteins via the p38alpha mitogen-activated protein kinase pathway during ischemia-reperfusion lung injury. J. Biol. Chem. *278*, 1248–1258.

Zuckerbraun, B.S., Billiar, T., Otterbein, S., Kim, P., Liu, F., Choi, A., Bach, F., and Otterbein, L.E. (2003). Carbon monoxide protects against liver failure through nitric oxide-induced heme oxygenase 1. J. Exp. Med. *198*, 1707–1716.